PERGAMON

Computers and Structures 80 (2002) 1477–1488

Computers & Structures

www.elsevier.com/locate/compstruc

Local quality of smoothening based a-posteriori error estimators for laminated plates under transverse loading

P.M. Mohite, C.S. Upadhyay *

Department of Aerospace Engineering, Indian Institute of Technology, Kanpur 208016, India

Received 26 July 2001; accepted 4 May 2002

Abstract

The local and global quality of various smoothening based a-posteriori error estimators is tested in this paper, for symmetric laminated composite plates subjected to transverse loads. Smoothening based on strain recovery and displacement-field recovery is studied here. Effect of ply orientation, laminate thickness, boundary conditions, mesh topology, and plate model is studied for a rectangular plate. It is observed that for interior patches of elements, both the estimators based on strain or displacement smoothening are reliable. For element patches at the boundary of the domain, all estimators tend to be unreliable (especially for angle-ply laminates). However, the strain recovery based estimator is clearly more robust for element patches at the boundary, as compared to displacement-recovery based error estimators. Globally, all the estimators tested here were found to be very robust.

Keywords: Laminated composite; Plates; Finite element; Hierarchic plates; Strain recovery; Displacement recovery; A-posteriori error

1. Introduction

With the advent of several new materials, and improved manufacturing capabilities, composites are replacing metals in the fabrication of a number of engineering components. Lightweight, high-speed structures are increasingly becoming composite based. Thus, development of appropriate analysis and design tools for composite structures is essential. The use of finite element methods in the analysis of laminated composite structures is prevalent, especially for plate or shell type structures made of unidirectional composites. Several authors have used the finite element analysis in the optimal design of structures made of composites (see [1] for details). The critical constraint quantities (e.g. maximal stress, buckling load, natural frequency, etc.) have to be obtained accurately, for the design to be reliable. This requires an adaptive finite element analysis, with control of the error in the various desired response quantities. An a-posteriori estimate of the error in the desired response quantity employs the standard local error estimators (see [2] for details). In order to have complete confidence in the computed solution quantities, reliability of the error estimator is essential, both at the local and global levels.

In [3] a comprehensive computational approach for the determination of the asymptotic quality of a-posteriori error estimators was presented, for the Poisson equation and the planar elasticity problem (with orthotropic material). It was found that the local quality of error estimators depends on several factors, e.g. mesh topology, material parameters, loading data and boundary-conditions. It was found in [3–5] that the error estimator based on stress recovery (defined in [6]) was reliable. It should be noted that, as compared to residual type error estimators (see [3,4]), the smoothening type

* Corresponding author.
E-mail address: shekhar@iitk.ac.in (C.S. Upadhyay).

0045-7949/02/$ - see front matter
PII: S0045-7949(02)00099-8

estimators tend to be more economical because the size of the local problems to be solved is smaller.

In [7] it was observed that for laminated composite plates the quality of the error estimators also depends on the lamina material properties, ply orientation, ply stacking sequence, the number of laminae and the laminate thickness. The effect of the particular plate model should also be analyzed. Several higher order plate theories have been proposed in the literature (see [8–15]), for the analysis of laminated plates and shells. Obviously, a proper analysis of these structures would require simultaneous control of modeling (with respect to three-dimensional elasticity) and discretisation error (see [16–24] and the references therein). Here, we do not address the issue of a-posteriori control of modeling error (see [15] for an example). The plate model will be fixed in this study, and the discretisation error will be measured with respect to the exact solution of the plate model. In [7] a reliable strain recovery based error estimator was presented, for laminated composite plates. It was found in [7] that the performance of the strain recovery based estimator (defined later) is reasonably robust. In the interior of the mesh, the estimator was very reliable, in the absence of boundary-layers and locking influence. At the boundary, the elementwise quality deteriorated. Globally, the estimator studied in [7] was found to be very reliable. In the current study, several alternative versions of smoothening based error estimators will be presented. A detailed analysis of the quality of these error estimators will also be carried out.

2. Plate theory for laminates

Several plate theories are available in the literature. For all the plate theories displacement field is represented in terms of known functions in the thickness variable z (either as a power series representation, or a piecewise polynomial representation) as given by [8,9] and references therein. Let us define the generic displacement field as:

$$\mathbf{u}(x,y,z) = \begin{Bmatrix} u(x,y,z) \\ v(x,y,z) \\ w(x,y,z) \end{Bmatrix} = \boldsymbol{\Phi}\mathbf{U} \tag{1}$$

where

$$\boldsymbol{\Phi} = \begin{bmatrix} \Phi_1(z) & 0 & \Phi_3(z) & 0 & 0 & \Phi_6(z) & 0 & 0 & \Phi_9(z) & 0 & \cdots \\ 0 & \Phi_2(z) & 0 & \Phi_4(z) & 0 & 0 & \Phi_7(z) & 0 & 0 & \Phi_{10}(z) & \cdots \\ 0 & 0 & 0 & 0 & \Phi_5(z) & 0 & 0 & \Phi_8(z) & 0 & 0 & \cdots \end{bmatrix} \tag{2}$$

$$\mathbf{U}^{\mathbf{T}} = \{u_0, v_0, u_1, v_1, w_0, u_2, v_2, w_1, u_3, v_3, w_2, \dots\} \tag{3}$$

where all the components of $\mathbf{U}$ are functions of x and y.

Different plate models can be obtained by using specific representations of $\Phi_i(z)$. The plate model employed in the numerical study is given by (see [8])

$$\Phi_1(z) = \Phi_2(z) = \Phi_5(z) = 1, \quad \Phi_3(z) = \Phi_4(z) = z,$$
$$\Phi_6(z) = \Phi_7(z) = z^3; \quad \Phi_i(z) = 0 \text{ for } i > 7 \tag{4}$$

Depending on the number of independent functions (represented as N_{MODEL}) employed in the representation of $\mathbf{U}(x,y,z)$, we get various higher order models. For example, in the representation used for the numerical study $N_{\mathrm{MODEL}} = 7$.

The laminate is made by stacking laminae with given material properties, orientation and ply thickness. For a given lamina 'l', the generalised Hooke's law (see [10,11]) gives:

$$\sigma^{(l)}(\mathbf{u}) = \bar{\mathbf{Q}}^{(l)}\varepsilon^{(l)}(\mathbf{u}) \tag{5}$$

where,
$\sigma^{l}(\mathbf{u}) = \{\sigma^{l}_{xx}(\mathbf{u}), \sigma^{l}_{yy}(\mathbf{u}), \sigma^{l}_{zz}(\mathbf{u}), \sigma^{l}_{zy}(\mathbf{u}), \sigma^{l}_{zx}(\mathbf{u}), \sigma^{l}_{xy}(\mathbf{u})\}^{\mathrm{T}}$ is the engineering stress vector for the lth lamina; $\varepsilon^{(l)}(\mathbf{u}) = \{\varepsilon^{(l)}_{xx}(\mathbf{u}), \varepsilon^{(l)}_{yy}(\mathbf{u}), \varepsilon^{(l)}_{zz}(\mathbf{u}), \gamma^{(l)}_{yz}(\mathbf{u}), \gamma^{(l)}_{xz}(\mathbf{u}), \gamma^{(l)}_{xy}(\mathbf{u})\}^{\mathrm{T}}$ is the engineering strain vector for the lth lamina; $\bar{\mathbf{Q}}^{(l)}$ is the material matrix for the lth lamina (transformed to the x–y coordinate system). Using the definition of $\varepsilon^{(l)}$ in terms of the displacement field $\mathbf{u}(x,y,z)$, the strain energy $\mathscr{U}$, and the potential $\mathscr{V}$ due to the transverse loads acting on the top and bottom faces of the plate are:

$$\mathscr{U}(\mathbf{u}) = \frac{1}{2}\int_{\Omega} \sigma(\mathbf{u})\varepsilon(\mathbf{u})\,\mathrm{d}V = \frac{1}{2}\int_{\Omega_{2\mathrm{D}}} \left(\sum_{i=1}^{N_{\mathrm{LAY}}} \int_{z_{i-1}}^{z_i} (\sigma^{(l)}(\mathbf{u})\varepsilon^{(l)}(\mathbf{u})\,\mathrm{d}z) \right) \mathrm{d}A \tag{6}$$

$$\mathscr{V}(\mathbf{u}) = \int_{R^+} q^+ w_0\,\mathrm{d}A + \int_{R^-} q^- w_0\,\mathrm{d}A \tag{7}$$

Here Ω is the plate domain of interest (of rectangular cross section $\Omega_{2\mathrm{D}} = \{(x,y) | 0 \leqslant x \leqslant a, 0 \leqslant y \leqslant b\}$ and depth d), as shown in Fig. 1a; N_{LAY} is the number of laminae; z_i are the z coordinates of interlaminar interfaces (as shown in Fig. 1b); R^+ and R^- are the top and bottom faces of the plate, respectively; $q^+(x,y)$ and $q^-(x,y)$ are the transverse loads on R^+ and R^-, respectively.

Thus, the total potential energy is given as:

$$\Pi(\mathbf{u}) = \mathscr{U}(\mathbf{u}) - \mathscr{V}(\mathbf{u}) \tag{8}$$

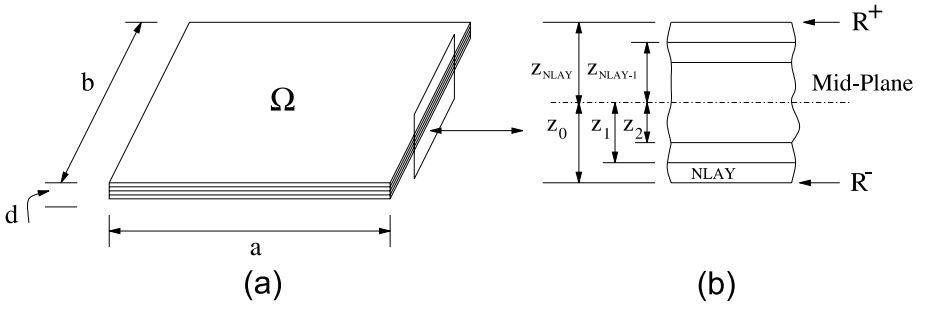

Fig. 1. Plate domain with interlaminar interfaces and top and bottom faces.

Minimizing $\Pi(\mathbf{u})$ with respect to $\mathbf{u}$, we get

$$\mathscr{B}(\mathbf{u},\delta\mathbf{u}) = \int_{\Omega_{2D}} \sum_{i=1}^{N_{LAY}} \int_{z_{i-1}}^{z_i} (\sigma^{(l)}(\mathbf{u})\varepsilon^{(l)}(\delta\mathbf{u})\,\mathrm{d}z)\,\mathrm{d}A = \mathscr{F}(\delta\mathbf{u}) = \int_{R^+} q^+\delta w_0\,\mathrm{d}A + \int_{R^-} q^-\delta w_0\,\mathrm{d}A \quad (9)$$

The variational formulation (9) is often written in its equivalent form in terms of stress resultants at the central surface Ω_{2D} of the plate. The above formulation leads to N_{MODEL} number of coupled equation in terms of the independent functions used in the representation (1). The finite element formulation of the above problem follows by replacing the given functions by the approximating series representation in terms of the basis functions. Here we will take elementwise p order approximation for all the unknown functions.

3. Definition of a-posteriori error estimator based on strain recovery and displacement recovery

Let $\mathbf{u}_{FE}$ be the finite element solution and $\varepsilon(\mathbf{u}_{FE})$ the corresponding strain components. The a-posteriori estimation of the error is based on the recovery of a smoothened strain field ε^*, or displacement field $\mathbf{u}^*$, by postprocessing $\mathbf{u}_{FE}$. This recovered strain or displacement field is used to define the element error indicator η_τ, which for the element τ is given as:

$$\eta_\tau^2 = \int_\tau \left(\sum_{i=1}^{N_{LAY}} \int_{z_{i-1}}^{z_i} ((\varepsilon^* - \varepsilon(\mathbf{u}_{FE}))\bar{\mathbf{Q}}^{(i)}(\varepsilon^* - \varepsilon(\mathbf{u}_{FE})))\,\mathrm{d}z \right) \mathrm{d}A \quad (10)$$

where ε^* is obtained either by directly recovering a strain field, or from the recovered displacement field $\mathbf{u}^*$. Several postprocessing procedures are possible (see [6,12, 13]). The postprocessing procedures employed in this study are:

3.1. Estimator based on strain recovery (EST1)

For each element τ, a polynomial strain field $\varepsilon^* \in \mathscr{P}_\varepsilon(\tau)$ is recovered, by using an energy projection of the finite element strain, $\varepsilon(\mathbf{u}_{FE})$, over a one-layer neighbourhood of τ (given as patch P_τ as shown in Fig. 2). This can be represented as:

For element τ, find $\varepsilon^* \in \mathscr{P}_\varepsilon(\tau)$ which minimizes

$$J_{\varepsilon^*} = \frac{1}{2} \sum_{\bar{\tau}\in P_\tau} \sum_{l=1}^{N_{LAY}} \int_{A_{\bar{\tau}}} \int_{z_{l-1}}^{z_l} (\varepsilon^* - \varepsilon(\mathbf{u}_{FE}))\mathbf{Q}^{(l)} \times (\varepsilon^* - \varepsilon(\mathbf{u}_{FE}))\,\mathrm{d}z\,\mathrm{d}A \quad (11)$$

where $\mathscr{P}_\varepsilon(\tau) = \{\varepsilon | \varepsilon_{xx}, \varepsilon_{yy}, \gamma_{xy} \in S^p(P_\tau); \varepsilon_{zz}, \gamma_{xz}, \gamma_{yz} \in S^{p+1} \times (P_\tau)\}$, with $S^q(P_\tau)$ being the set of polynomials of order q over the patch P_τ.

3.2. Estimator based on displacement field recovery using energy projection (EST2 and EST3)

For each element τ a displacement field $\mathbf{u}^* = \Phi\mathbf{U}^*$, where $\mathbf{U}^* \in \mathscr{P}_u^{p+k}(\tau)$, is recovered using an energy

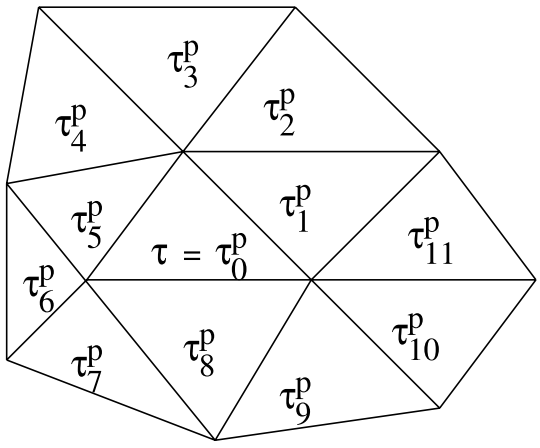

Fig. 2. An element τ with a layer of elements $\{\tau_i^p\}_{i=0}^{11}$ surrounding it, forming the patch P_τ.

projection of the finite element solution $\mathbf{u}_{\mathrm{FE}}$ over the patch P_τ. This can be represented as:

For each τ, find $\mathbf{U}^* \in \mathscr{P}_u^{p+k}(\tau)$ which minimizes

$$J_{\mathbf{U}^*} = \frac{1}{2}\sum_{\bar{\tau}\in P_\tau}\sum_{l=1}^{N_{\mathrm{LAY}}}\int_{A\bar{\tau}}\int_{z_{l-1}}^{z_l}(\varepsilon(\mathbf{u}^*)-\varepsilon(\mathbf{u}_{\mathrm{FE}}))\mathbf{Q}^{(l)}(\varepsilon(\mathbf{u}^*) - \varepsilon(\mathbf{u}_{\mathrm{FE}}))\,\mathrm{d}z\,\mathrm{d}A + \delta\sum_{\bar{\tau}\in P_\tau}\int_{A\bar{\tau}}|\mathbf{U}^*-\mathbf{U}_{\mathrm{FE}}|^2\,\mathrm{d}A$$

where δ is a small number ($\delta = 10^{-8}$ has been used in the study); $\mathscr{P}_u^{p+k}(\tau) = \{\mathbf{U}|U_i \in S^{p+k}(P_\tau),\ i = 1,2,\ldots N_{\mathrm{MODEL}}\}$; $\mathbf{u}_{\mathrm{FE}} = \Phi\mathbf{U}_{\mathrm{FE}}$.

The above definition is employed for all elements τ in the interior of the domain for both estimators EST2 and EST3. For EST2, the above definition is also employed for elements at the boundary. However, at boundaries with Dirichlet condition, one would like to impose the applied displacement boundary conditions stringently, while finding $\mathbf{U}^*$. Thus, in the case of EST3, for elements τ at the Dirichlet boundary, $\mathbf{U}^*$ is obtained by minimising:

$$J_{1,\mathbf{U}^*} = J^*_{\mathbf{U}} + \lambda\sum_{\bar{\tau}\in P_\tau}\int_{\partial\bar{\tau}\subseteq\Gamma_{\mathrm{D}}}|\mathbf{U}^*-\bar{\mathbf{U}}|^2\,\mathrm{d}s \tag{12}$$

where λ is a penalty parameter ($\lambda = 10^8$ was employed in the study); $\bar{\mathbf{U}}$ is the known boundary displacement, and Γ_{D} is the Dirichlet part of the boundary $\partial\Omega_{2\mathrm{D}}$ of the domain $\Omega_{2\mathrm{D}}$.

3.3. Estimator based on displacement field recovery using L_2 projection (EST4)

For each element τ a polynomial displacement field $\mathbf{U}^* \in \mathscr{P}_u^{p+k}(\tau)$ is recovered from the following minimisation problem:

For each τ, find $\mathbf{U}^* \in \mathscr{P}_u^{p+k}(\tau)$ which minimizes

$$J_{2,\mathbf{U}^*} = \frac{1}{2}\sum_{\bar{\tau}\in P_\tau}\int_{A_{\bar{\tau}}}|\mathbf{U}^*-\mathbf{U}_{\mathrm{FE}}|^2\,\mathrm{d}A \tag{13}$$

The estimator obtained with $p+1$ recovery will be referred to as EST4A, while the estimator obtained with $p+2$ recovery will be referred to as EST4B.

Remark 1. This recovery is a planar recovery, using the L_2 projection of each component of $\mathbf{U}_{\mathrm{FE}}$. This leads to very small matrix problems at the element level, with multiple right hand sides. Thus, this recovery is computationally inexpensive.

The detailed procedures for the construction of the various recovery based error estimators is given in the appendix.

The error estimators proposed here have to be tested for their reliability. Since the goal of all smoothening based error estimators is to get superconvergent stress or strain fields, an obvious choice for the measure of the base error (i.e. the desired "true" error) is given as $\mathbf{e} = \mathbf{u}_{\mathrm{FE}}^{(p+q)} - \mathbf{u}_{\mathrm{FE}}^{(p)}$, with $\mathbf{u}_{\mathrm{FE}}^{(k)}$ as the finite element solution with elements of order k.

Given the element error indicators η_τ, the global error estimator ξ_Ω is given as:

$$\xi_\Omega = \sqrt{\sum_{\tau=1}^{N_{\mathrm{EL}}}\eta_\tau^2} \tag{14}$$

where N_{EL} is the total number of elements in the mesh.

Thus, the "desired" error norm will be $|||\mathbf{e}|||_\Omega = \sqrt{2\mathscr{U}(\mathbf{e})}$, which will be used to obtain a measure of the quality of the error estimators, i.e.

$$\kappa_\Omega = \frac{\xi_\Omega}{|||\mathbf{e}|||_\Omega} \tag{15}$$

where κ_Ω is the global effectivity index (the ideal value of κ_Ω is 1). The local quality of an estimator will be obtained by finding the effectivity index for the patch ω of interest, i.e.

$$\kappa_\omega = \frac{\xi_\omega}{|||\mathbf{e}|||_\omega} \tag{16}$$

where $\xi_\omega = \sqrt{\sum_{\tau\in\omega}\eta_\tau^2}$, $|||\mathbf{e}|||_\omega = \sqrt{2\mathscr{U}_\omega(\mathbf{e})}$ with $\mathscr{U}_\omega(\mathbf{e})$ as the strain energy of the error in the patch ω.

4. Validation of the quality of a-posteriori error estimators

Several factors affect the local and global quality of a-posteriori error estimators. The major factors are:

1. effect of ply orientation, stacking sequence;
2. effect of number of laminae;
3. effect of boundary conditions and domain regularity;
4. effect of loading type;
5. effect of thickness of plate;
6. effect of plate model;
7. effect of polynomial order of the recovered field;
8. effect of mesh type.

The effect of all these factors on the local and global quality of a-posteriori error estimators will be studied through numerical examples. The material of interest will be T300/5208 Graphite/Epoxy (prepreg) with the following properties (as given in [26]):

$E_{ll} = 132.5$ GPa; $E_{tt} = 10.8$ GPa; $\nu_{lt} = 0.24$; $\nu_{tt} = 0.49$; $G_{lt} = 5.7$ GPa; $G_{tt} = 3.4$ GPa

For the numerical study, we will take the plate model given by (4). Further, we will consider only the following types of boundary conditions:

1. soft simple support ($u_t = w = 0$), called SS;
2. hard simple support ($u_n = w = 0$), called HSS;
3. clamped ($u_t = u_n = w = 0$),

where u_t and u_n are the in-plane tangential and normal displacement components, respectively (as shown in Fig. 3); w is the transverse displacement. Here, we will assume the same boundary condition type on all boundary edges.

Remark 2. Ideally, an analysis of the asymptotic quality of error estimators is desired (see [3,4]). Here, a sufficiently fine mesh (shown in Fig. 2) is employed, in order to get close to the asymptotic quality. Note that the preasymptotic quality (i.e. for coarse meshes) of all error estimators can be significantly different from that reported in this study. Study of the preasymptotic quality of the error estimators is also important, in order to assess the quality of the error prediction for the starting (coarse) mesh in an adaptive process.

Remark 3. The presence of strong boundary-layers in the solution can effect the quality of the overall finite element solution (and the error estimator), unless appropriate mesh refinement (see [14,25]) is done near the boundary. Here, we have not employed mesh refinements (h or p) to counter the influence of boundary-layer on the quality of error estimators. Suitable refinements at the boundary, will improve the observed quality of the error estimators further.

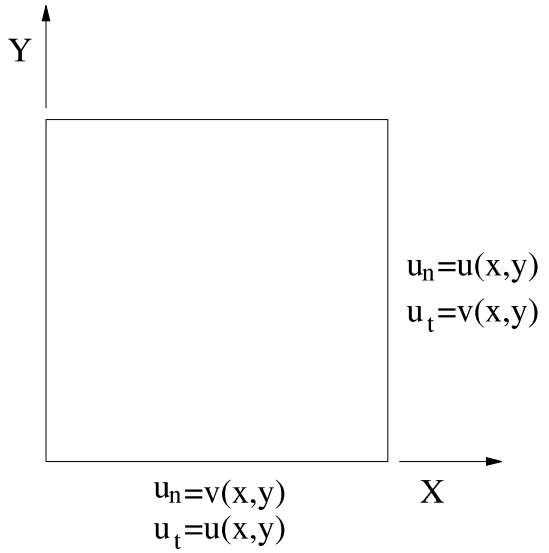

Fig. 3. Plate showing tangential and normal components of displacement on the edges.

Case 1: *Quality for element patches in the interior of the domain*, $\Omega_{2D,interior}$. The local performance of the error estimator has to be understood for the various possible scenarios separately. We know that the boundary layer effect in the finite element solution may be present only in few layers of elements adjoining the boundary. For elements removed from the boundary, the finite element solution behaves like the local best approximation, i.e. the local error converges at the optimal rate. Thus, the first check for the quality of the error estimator should be for elements in the interior of the domain, i.e. for element patches (various representative patches are shown in Fig. 5) in the subregion $\Omega_{2D,interior}$. In Fig. 4 the element patches at the boundary and interior are shown for the meshes used in this study.

All the numerical results presented will be for the four-layered laminates, unless otherwise specified, with the ply thickness fixed to $d_l = 0.127$ mm, $l = 1,2,3,\ldots N_{LAY}$. In Tables 1 and 2, the extremal values of the effectivity index (κ_{max}, and κ_{min} respectively), for the element patches ω in the interior of the domain (see Fig. 4) are given for various ply orientations and boundary conditions. Effect of plate thickness is accounted for by taking $\frac{a}{d} = 5$ (thick plate), 10 (moderately thick plate), 100 (thin plate). Elements of order $p = 2$ are taken for thick and moderately thick plates, Note that since we are interested in the asymptotic quality of error estimators, for thin plates $p = 3$ is employed in all cases (as for $p = 2$ the error is not asymptotic in nature). The transverse load is fixed to a uniformly distributed load of intensity $q^+ = 2$ N/mm^2 and $q^- = 0$.

From the results we observe that:

1. Estimators EST1, EST2 and EST4B are very reliable for patches in the interior of the domain, with $0.97 \leqslant \kappa_\omega \leqslant 1.07$.
2. The asymptotic quality of error estimators is relatively insensitive to the ply orientation, and plate thickness.
3. The effect of the boundary conditions is not seen in the interior patches. Hence, the boundary-layer in the numerical solution is localised to only one patch of elements, adjacent to the boundary i.e. elements in $\Omega_{2D,outer}$.
4. The estimator EST4A is not reliable ($0.98 \leqslant \kappa_\omega \leqslant 2.29$). Hence, L_2 projection with $(p+1)$ order polynomials is not advisable. EST4B ($\kappa_\omega \approx 1$) is very reliable in the interior. Hence, L_2 projection with $(p+2)$ order polynomials is more robust.
5. For interior patches EST2 and EST4B show similar behavior.

Thus, for interior patches EST4B is preferable because it is very robust and the computational cost is negligible, as compared to EST1 and EST2.

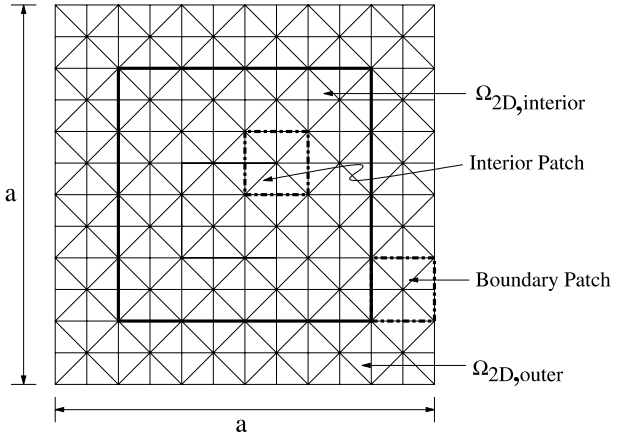

Fig. 4. The square plate of dimensions $a \times a$, with the mesh shown. The layer of element patches adjacent to the boundary are given by $\Omega_{2D,outer}$. All other patches lie in subdomain $\Omega_{2D,interior}$. Sample inner and boundary patches are also shown (with dashed border).

Table 1
Quality of error estimators for patches in $\Omega_{2D,interior}$: uniform transverse load ($q^+ = 2$ N/mm^2) $[0/90]_s$ laminate

$\frac{a}{d}$ ratio	Estimator	SSS		HSS		Clamped	
		κ_{min}	κ_{max}	κ_{min}	κ_{max}	κ_{min}	κ_{max}
5	EST1	1.0056	1.0056	1.0175	1.0175	1.0173	1.0173
	EST2	0.9989	0.9989	1.0015	1.0015	1.0014	1.0014
	EST4A	1.0365	1.0365	1.0609	1.0609	1.0604	1.0604
	EST4B	0.9954	0.9954	0.9978	0.9978	0.9976	0.9976
10	EST1	1.0053	1.0053	1.0230	1.0230	1.0231	1.0231
	EST2	1.0014	1.0014	1.0045	1.0045	1.0046	1.0046
	EST4A	1.0713	1.0713	1.1178	1.1178	1.1176	1.1176
	EST4B	1.0003	1.0003	0.9998	0.9998	0.9997	0.9997
100	EST1	1.0025	1.0025	1.0230	1.0230	1.0231	1.0231
	EST2	1.0013	1.0013	0.9958	0.9958	0.9957	0.9957
	EST4A	1.1539	1.1539	1.7105	1.7105	1.7105	1.7105
	EST4B	0.9843	0.9843	0.9789	0.9789	0.9789	0.9789

Table 2
Quality of error estimators for patches in $\Omega_{2D,interior}$: uniform transverse load ($q^+ = 2$ N/mm^2) $[45/-45]_s$ laminate

$\frac{a}{d}$ ratio	Estimator	SSS		HSS		Clamped	
		κ_{min}	κ_{max}	κ_{min}	κ_{max}	κ_{min}	κ_{max}
5	EST1	1.0203	1.0547	1.0137	1.0719	1.0144	1.0175
	EST2	0.9657	0.9753	0.9807	0.9933	0.9945	0.9986
	EST4A	1.0243	1.0413	1.0419	1.1165	1.0555	1.0855
	EST4B	0.9651	0.9671	0.9755	1.0111	0.9985	1.0025
10	EST1	0.9848	0.9896	0.9892	0.9900	1.0153	1.0193
	EST2	0.9589	0.9777	0.9628	0.9692	0.9959	1.0011
	EST4A	1.0463	1.0469	1.0672	1.1733	1.0919	1.2109
	EST4B	0.9716	0.9743	0.9633	0.9844	0.9888	1.0195
100	EST1	0.9272	0.9307	0.9156	0.9358	0.9900	1.0011
	EST2	0.9305	0.9393	0.9066	0.9243	0.9774	0.9911
	EST4A	0.9863	1.1679	1.3676	2.2956	1.4543	2.5316
	EST4B	0.9217	0.9252	0.9218	0.9323	0.9864	1.0080

Case 2: *Quality for element patches in the boundary region*, $\Omega_{2D,outer}$. The local quality of the proposed error estimators are investigated separately for element patches in $\Omega_{2D,outer}$. From the results given in Tables 3 and 4, we observe that:

1. Estimator EST1 is reliable upto the boundary for all $\frac{a}{d}$ ratios and symmetric cross-ply ($[0/90]_s$), with $0.86 \leqslant \kappa_\omega \leqslant 1.04$.
2. For the angle-ply laminate ($[45/-45]_s$), the quality of EST1 deteriorates with $0.73 \leqslant \kappa_\omega \leqslant 1.70$.
3. For $[0/90]_s$ laminate with soft simply supported boundary condition, estimators EST1, EST3, EST4B are robust upto the boundary.
4. Estimator EST3 is better than estimator EST2 for boundary patches. Thus, explicit imposition of the essential boundary conditions is necessary, for the displacement recovery method, in order to get reliable error estimators.
5. Estimator EST4B is more reliable than EST3. Hence, for the class of problems considered here, estimator EST4B is preferable to EST3.
6. All estimators can significantly underestimate the error, with $\kappa_{min} \approx 0.6$.

It should be noted that the patches at the boundary correspond to one layer of elements at the domain boundary. Hence, the inferior performance of the

Table 3
Quality of error estimators for patches in $\Omega_{2D,outer}$: uniform transverse load ($q^+ = 2$ N/mm^2); $[0/90]_s$ laminate

$\frac{a}{d}$ ratio	Estimator	SSS		HSS		Clamped	
		κ_{min}	κ_{max}	κ_{min}	κ_{max}	κ_{min}	κ_{max}
5	EST1	0.9981	1.0456	0.9668	1.1268	0.9655	1.1195
	EST2	0.9767	1.0211	0.8442	1.0229	0.8468	1.0227
	EST3	0.9838	1.1042	0.8558	1.0229	0.8564	1.0631
	EST4A	0.9699	1.1439	0.9097	1.1262	0.9117	1.1602
	EST4B	0.9621	1.0544	0.8596	1.0086	0.8617	1.0081
10	EST1	0.9845	1.0286	0.8744	1.0691	0.8737	1.0692
	EST2	0.9737	1.0053	0.7988	1.0128	0.8007	1.0128
	EST3	0.9813	1.0293	0.8132	1.0128	0.8564	1.0631
	EST4A	0.9690	1.1186	0.8621	1.2280	0.8633	1.2255
	EST4B	0.9616	1.0382	0.8105	0.9997	0.8124	0.9997
100	EST1	0.9718	1.0209	0.8604	1.0357	0.8617	1.0358
	EST2	0.9689	1.0294	0.6988	1.0178	0.7015	1.0178
	EST3	0.9715	1.0572	0.7211	1.0616	0.7239	1.0853
	EST4A	1.4484	2.6835	1.7091	3.4468	1.4028	3.4483
	EST4B	0.9812	1.3339	0.8395	1.1053	0.7024	1.1035

Table 4
Quality of error estimators for patches in $\Omega_{2D,outer}$: uniform transverse load ($q^+ = 2$ N/mm^2); $[45/-45]_s$ laminate

$\frac{a}{d}$ ratio	Estimator	SSS		HSS		Clamped	
		κ_{min}	κ_{max}	κ_{min}	κ_{max}	κ_{min}	κ_{max}
5	EST1	0.9703	1.7028	0.9462	1.6029	0.9521	1.2558
	EST3	0.8605	2.0219	0.7995	1.8825	0.8356	1.8446
	EST4A	0.9118	1.8953	0.8611	1.7498	0.8911	1.2967
	EST4B	0.8576	1.7705	0.8094	1.6602	0.8445	1.1505
10	EST1	0.8803	1.5212	0.8212	1.2944	0.8673	1.1035
	EST3	0.7796	1.8136	0.7259	1.4505	0.7861	1.5711
	EST4A	0.8557	1.6777	0.7795	1.3885	0.8396	1.3133
	EST4B	0.7651	1.5078	0.7183	1.2323	0.7867	1.0195
100	EST1	0.7331	1.2225	0.8257	1.0354	0.9258	1.0325
	EST3	0.5706	1.5167	0.6118	1.2022	0.8124	1.4295
	EST4A	0.9980	4.0447	0.9276	3.6262	1.4791	3.9337
	EST4B	0.6136	1.3099	0.6111	1.1072	0.8378	1.2803

estimators (with respect to interior patches) is restricted to a small region abutting the boundary.

Remark 4. Though the global effectivity index has not been reported here, it was found that $0.86 \leqslant \kappa_\Omega \leqslant 1.2$ for estimators EST1, EST3 and EST4B. Hence, all the estimators are *globally very reliable*. This is essential for an accurate stopping criterion for an adaptive process.

Case 3: *Effect of number of laminae*. The effect of increasing number of laminae constituting the laminate is studied by taking 4, 8 and 16 ply laminate. The stacking sequences for these laminates are $[0/90]_s$, $[0/90]_{s_2}$ and $[0/90]_{s_4}$, respectively. Here, the goal is to study the effect of the number of plies on the local quality of the error estimators for the worst-case scenario obtained from the previous examples. Thus, we consider the plate with clamped boundaries. The results are presented in Tables 5 and 6.

From the results we can observe that:

1. Estimators EST1 and EST3 are reliable for interior element patches, for any number of plies.

Table 5
Effect of number of plies for $\Omega_{2D,interior}$; cross-ply laminate; clamped support

$\frac{a}{d}$ ratio	N_{LAY}	EST1		EST2	
		κ_{min}	κ_{max}	κ_{min}	κ_{max}
5	4	1.0173	1.0173	1.0014	1.0014
	8	1.0117	1.0117	1.0013	1.0013
	16	1.0134	1.0134	1.0017	1.0017
10	4	1.0231	1.0231	1.0046	1.0046
	8	1.0165	1.0165	1.0035	1.0035
	16	1.0174	1.0174	1.0039	1.0039
100	4	1.0231	1.0231	0.9957	0.9957
	8	1.0215	1.0215	1.0023	1.0023
	16	1.0211	1.0211	1.0034	1.0034

Table 6
Effect of number of plies for $\Omega_{2D,outer}$; cross-ply laminate; clamped support

$\frac{a}{d}$ ratio	N_{LAY}	EST1		EST3	
		κ_{min}	κ_{max}	κ_{min}	κ_{max}
5	4	0.9655	1.1195	0.8564	1.0631
	8	0.9767	1.1534	0.8424	1.0761
	16	1.0143	1.1076	0.8632	1.1127
10	4	0.8737	1.0692	0.8137	1.0128
	8	0.8690	1.0463	0.7719	1.0102
	16	0.9070	1.0483	0.8020	1.0754
100	4	0.8617	1.0358	0.7239	1.0853
	8	0.8829	1.0152	0.7814	1.0847
	16	0.9132	1.0158	0.8293	1.0915

2. For the boundary patches EST1 is more reliable, as compared to EST2.
3. The reliability of the estimators improves with increasing number of laminae.

Case 4: *Influence of mesh topology*. For triangular elements, the topology of the elements can affect quality of the error estimation (see [3] for details). In order to study the influence of the mesh topology, we consider meshes formed by repetition of the periodic patterns shown in Fig. 5.

Here, we take the thin plate ($\frac{a}{d} = 100$) with clamped boundaries. In Table 7, we give some values of κ_{max} and κ_{min} obtained for meshes of Regular type, Criss-Cross type along with the Union Jack type (which is employed in all the numerical studies reported above) for the $[0/90]_s$ laminate. From the results we note that:

1. For $\Omega_{2D,interior}$, the estimators EST1 and EST3 are accurate for all mesh patterns, and relatively insensitive to mesh topology.
2. For $\Omega_{2D,outer}$, estimator EST1 is more accurate compared to EST3 for all patterns.
3. The effect of the mesh topology is clearly observable for mesh patches at the boundary of the domain. For the Criss-Cross pattern all estimators seem to be more robust at the boundary ($0.91 \leqslant \kappa_\omega \leqslant 1.15$), as compared to other patterns (e.g. for the Regular pattern $0.62 \leqslant \kappa_\omega \leqslant 1.14$).

Case 5: *Effect of polynomial order of recovered field*. The quality of estimator based on smoothening depends on the order of polynomials employed in the fitting. Often, $p+1$ fitting is used for recovered displacement field, and p order polynomials are used for strain (or stress) recovery (see [6]). Here, we analyze the effect of the order of the recovered field for the L_2 projection based estimator. EST4A is obtained by using $p+1$ order displacement fitting and EST4B is obtained using $p+2$ order fitting. From Tables 1 and 2 we observe that:

1. EST4B is more accurate than EST4A for interior patches in cross-ply laminate. EST4A tends to overestimate the error, with the quality deteriorating with the $\frac{a}{d}$ ratio. However, EST4B is relatively insensitive to the $\frac{a}{d}$ ratio.
2. For boundary patches, EST4A is unreliable with $\kappa_{max} > 4$. However, for EST4A $\kappa_{min} > 0.85$, while EST4B can have $\kappa_{min} \approx 0.6$. Thus, EST4B can significantly underestimate the error while EST4A can severly overestimate the error.

A similar performance is observed for EST3 with $p+1$ or $p+2$ order fitting, and hence is not reported here. Overall, recovery of displacement with $(p+2)$

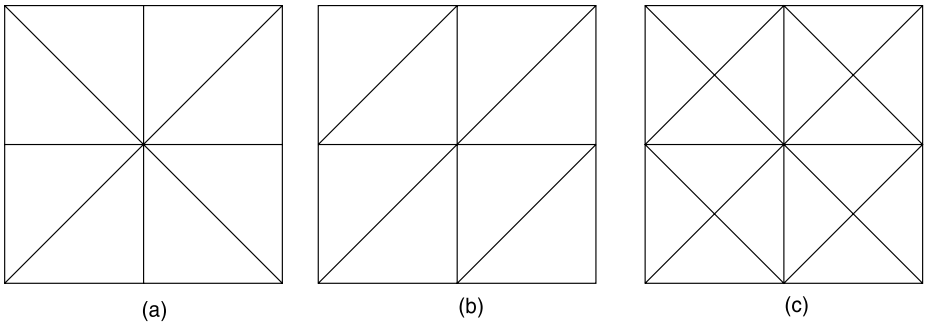

Fig. 5. The periodic patterns representing a patch of elements: (a) Union Jack; (b) Regular; (c) Criss-Cross.

Table 7
Effect of mesh topology on quality of error estimators for $[0/90]_s$ laminate; $\frac{a}{d} = 100$; clamped support

Mesh pattern	Estimator	$\Omega_{2D,interior}$		$\Omega_{2D,outer}$	
		κ_{min}	κ_{max}	κ_{min}	κ_{max}
Regular	EST1	1.0228	1.0230	0.7614	1.0473
	EST3	1.0074	1.0074	0.6249	1.1401
Union Jack	EST1	1.0231	1.0231	0.8617	1.0358
	EST3	0.9957	0.9957	0.7239	1.0853
Criss-Cross	EST1	1.0238	1.0238	0.9501	1.1534
	EST3	1.0271	1.0271	0.9147	1.0911

order polynomials is preferable, as compared to $(p+1)$ order polynomials.

Case 6: *Effect of plate model*. In order to find out whether different definitions of the higher order plate model can lead to dramatic changes in the observed quality of the smoothening-based error estimators, we consider here the hierarchic plate models proposed in [14]. For the eight-field model of [14], we report the extremal values of the patchwise effectivity index, for the displacement-recovery based error estimators, for various ply orientations for the thin plate ($\frac{a}{d} = 100$). Here, we consider the plate with either clamped or soft simply supported boundary edges. From the results reported in Table 8 we observe that:

1. Estimators EST3 and EST4B are very robust for interior mesh patches, ($0.88 \leqslant \kappa_\Omega \leqslant 1.16$).
2. For the boundary patches, both estimators become less robust, with $0.7 \leqslant \kappa_\Omega \leqslant 1.62$.
3. The observed quality of the estimators is identical to that reported for the conventional higher order plate theory given by (4).

Thus, the quality of the smoothening-based error estimators is independent of the plate theory employed.

Table 8
Effect of plate model on quality of error estimators; 8-field hierarchic model of [14]; $\frac{a}{d} = 100$

Laminate	Boundary condition	Estimator	$\Omega_{2D,interior}$		$\Omega_{2D,outer}$	
			κ_{min}	κ_{max}	κ_{min}	κ_{max}
$[0/90]_s$	SSS	EST3	0.960	0.960	0.981	1.000
		EST4B	1.105	1.105	1.180	1.620
	Clamped	EST3	0.984	1.008	0.824	0.939
		EST4B	1.149	1.149	1.001	1.094
$[0/45]_s$	SSS	EST3	0.944	0.964	0.918	1.001
		EST4B	1.073	1.076	1.106	1.493
	Clamped	EST3	0.907	1.008	0.772	0.950
		EST4B	1.100	1.105	1.001	1.131
$[-45/45]_s$	SSS	EST3	0.889	0.943	0.714	0.955
		EST4B	0.977	1.159	0.743	1.168
	Clamped	EST3	0.883	0.961	0.709	1.001
		EST4B	1.024	1.222	0.852	1.549

5. Conclusions

In this paper, a comprehensive study of the quality of several smoothening-based a-posteriori error estimators has been carried out for the rectangular laminated plate with symmetric ply stacking. The influence of various factors on the local and global qualities of all the error estimators has been studied. From the results, we can conclude the following:

1. Estimators EST1, EST3 and EST4B are very reliable for interior patches of elements for all mesh topologies.
2. At the boundary, estimator EST1 is the most robust amongst all the estimators, for the classes of meshes, boundary conditions, materials and plate thickness considered.
3. For angle-ply laminates, the estimators are less robust at the boundary, as compared to cross-ply laminates.
4. Explicit imposition of the applied Dirichlet boundary conditions, in the recovered displacement field, improves the quality of the estimator EST3 (as compared to estimator EST2).
5. For the soft simple support, the estimators are more robust as compared to the hard simple support or clamped type of boundary conditions.
6. The behavior of the estimators is relatively insensitive to the higher order plate model used.
7. With increased number of laminae in the plate, all the estimators show a slight improvement in the quality, especially at the boundary.
8. For the displacement-based recovery procedure, $p+2$ order recovery is preferable, as compared to $p+1$ order recovery.
9. For boundary patches, the effect of mesh topology on the quality of the error estimators is significant. For the Criss-Cross pattern, all the estimators are robust upto the boundary, while for the Regular pattern the underestimation can be severe.
10. Estimators EST1, EST3 and EST4B are very robust globally.
11. A locally robust and economical version of the smoothening-based error estimator can be obtained by using EST4B for all elements in the interior of the domain, and EST1 for the elements adjacent to the domain boundary.

Acknowledgements

The partial support of AR&DB under the research grant *Aero/RD-124/100/10/99-2000/1051* and Respond (ISRO), under the grant *10/3/370* are gratefully acknowledged by the second author.

Appendix A. Estimator based on strain recovery (EST1)

The strain field is taken to be of the same form as that corresponding to the exact solution of the plate model. For simplicity, let us consider the plate model given by (4). For other models the generic representation similar to (1) has to be employed.

Following the representation of the solution by (4), we get the components of strain as:

$$\varepsilon = \begin{Bmatrix} \varepsilon_{xx} \\ \varepsilon_{yy} \\ \gamma_{yz} \\ \gamma_{xz} \\ \gamma_{xy} \end{Bmatrix} = \begin{Bmatrix} \varepsilon^0_{xx} \\ \varepsilon^0_{yy} \\ \gamma^0_{yz} \\ \gamma^0_{xz} \\ \gamma^0_{xy} \end{Bmatrix} + z \begin{Bmatrix} \varepsilon^1_{xx} \\ \varepsilon^1_{yy} \\ 0 \\ 0 \\ \gamma^1_{xy} \end{Bmatrix} + z^2 \begin{Bmatrix} 0 \\ 0 \\ \gamma^1_{yz} \\ \gamma^1_{xz} \\ 0 \end{Bmatrix} + z^3 \begin{Bmatrix} \varepsilon^2_{xx} \\ \varepsilon^2_{yy} \\ 0 \\ 0 \\ \gamma^2_{xy} \end{Bmatrix}$$

The recovered strain ε^* is also assumed to have the same form (in terms of z) as the exact one. Thus, the recovered strain is also represented as:

$$\varepsilon^* = \begin{Bmatrix} \varepsilon^*_{xx} \\ \varepsilon^*_{yy} \\ \gamma^*_{yz} \\ \gamma^*_{xz} \\ \gamma^*_{xy} \end{Bmatrix} = \begin{Bmatrix} \varepsilon^{*,0}_{xx} \\ \varepsilon^{*,0}_{yy} \\ \gamma^{*,0}_{yz} \\ \gamma^{*,0}_{xz} \\ \gamma^{*,0}_{xy} \end{Bmatrix} + z \begin{Bmatrix} \varepsilon^{*,1}_{xx} \\ \varepsilon^{*,1}_{yy} \\ 0 \\ 0 \\ \gamma^{*,1}_{xy} \end{Bmatrix} + z^2 \begin{Bmatrix} 0 \\ 0 \\ \gamma^{*,1}_{yz} \\ \gamma^{*,1}_{xz} \\ 0 \end{Bmatrix} + z^3 \begin{Bmatrix} \varepsilon^{*,2}_{xx} \\ \varepsilon^{*,2}_{yy} \\ 0 \\ 0 \\ \gamma^{*,2}_{xy} \end{Bmatrix}$$

Given the representation of ε^*, it is now desired to obtain the recovered strain field as a polynomial element by element, such that the recovered strain components are polynomials that are one order higher than the corresponding finite element strain components. Thus, if elements of order p are employed all the recovered in-plane strain components are polynomials of degree p and the out of plane strain components are polynomials of degree $p+1$, and are given by:

$$\varepsilon_{xx}^{*,i} = \sum_{j=1}^{N_{IN}} \varepsilon_{xx,j}^{*,i} q_j(\hat{x},\hat{y}) \quad i = 0,1,2$$

$$\varepsilon_{yy}^{*,i} = \sum_{j=1}^{N_{IN}} \varepsilon_{yy,j}^{*,i} q_j(\hat{x},\hat{y}) \quad i = 0,1,2$$

$$\gamma_{yz}^{*,i} = \sum_{j=1}^{N_{OUT}} \gamma_{yz,j}^{*,i} q_j(\hat{x},\hat{y}) \quad i = 0,1$$

$$\gamma_{xz}^{*,i} = \sum_{j=1}^{N_{OUT}} \gamma_{xz,j}^{*,i} q_j(\hat{x},\hat{y}) \quad i = 0,1$$

$$\gamma_{xy}^{*,i} = \sum_{j=1}^{N_{IN}} \gamma_{xy,j}^{*,i} q_j(\hat{x},\hat{y}) \quad i = 0,1,2$$

where $N_{IN} = (p+1)(p+2)/2$, $N_{OUT} = (p+2)(p+3)/2$ and $q_j(\hat{x},\hat{y})$ are the monomials given by:

$$q_1(\hat{x},\hat{y}) = 1, \quad q_2(\hat{x},\hat{y}) = \hat{x}, \quad q_3(\hat{x},\hat{y}) = \hat{y},$$
$$q_4(\hat{x},\hat{y}) = \hat{x}^2, \; q_5(\hat{x},\hat{y}) = \hat{x}\hat{y}, \quad q_6(\hat{x},\hat{y}) = \hat{y}^2, \ldots$$

Here $\hat{x} = x - x_c^\tau$, $\hat{y} = y - y_c^\tau$ are the local coordinates with the origin at the centroid of the element of interest, τ.

A.1. Estimator based on displacement field recovery using energy projection (EST2 and EST3)

Here, the recovered displacement field is assumed to be of the same form as given by the solution (4). Thus, the recovered displacement field $\mathbf{U}^*$ is represented as:

$$\mathbf{U}^*(x,y,z) = \begin{Bmatrix} u^*(x,y,z) \\ v^*(x,y,z) \\ w^*(x,y,z) \end{Bmatrix} = \begin{Bmatrix} u_0^*(x,y) \\ v_0^*(x,y) \\ w_0^*(x,y) \end{Bmatrix} + z \begin{Bmatrix} u_1^*(x,y) \\ v_1^*(x,y) \\ 0 \end{Bmatrix} + z^3 \begin{Bmatrix} u_2^*(x,y) \\ v_2^*(x,y) \\ 0 \end{Bmatrix}$$

Given the representation for recovered displacement field $\mathbf{U}^*$, the recovered displacement field is obtained as a polynomial element by element, such that the recovered displacement components are polynomials that are k order higher than the finite element displacement components. Thus, if elements of order p are employed all the displacement components are polynomials of degree $p+k$, and are given as:

$$u^{*,i} = \sum_{j=1}^{NP} u_{,j}^{*,i} q_j(\hat{x},\hat{y}) \quad i = 0,1,2$$

$$v^{*,i} = \sum_{j=1}^{NP} v_{,j}^{*,i} q_j(\hat{x},\hat{y}) \quad i = 0,1,2$$

$$w^* = \sum_{j=1}^{NP} w_{,j}^{*} q_j(\hat{x},\hat{y})$$

where $NP = (p+k+1)(p+k+2)/2$ and $q_j(\hat{x},\hat{y})$ are the monomials as given previously.

A.2. Estimator based on displacement field recovery procedure using L_2 projection (EST4)

In this recovery procedure, the recovered displacement field is also assumed to be of the same form as given by the solution (4) and is as given above for EST3.

References

[1] Gürdal Z, Haftka RT, Hajela P. Design and optimization of laminated composite materials. New York: John Wiley & Sons Inc; 1999.

[2] Babuska I, Strouboulis T, Upadhyay CS, Gangaraj SK. A posteriori estimation and adaptive control of the pollution error in the *h*-version of the finite element method. Int J Numer Meth Eng 1995;38:4207–35.

[3] Babuska I, Strouboulis T, Upadhyay CS. A model study of the quality of a posteriori error estimators for linear elliptic problems. Error estimation in the interior of patchwise uniform grids of triangles. Comput Meth Appl Mech Eng 1994;114:307–78.

[4] Babuska I, Strouboulis T, Upadhyay CS, Gangaraj SK, Copps K. Validation of a posteriori error estimators by numerical approach. Int J Numer Meth Eng 1994;37:1073–123.

[5] Upadhyay CS. Computer-based analysis of error estimation and superconvergence in finite element computations. Ph. D. dissertation at Texas A&M University, Texas, May 1997.

[6] Zhu JZ, Zienkiewicz OC. Superconvergence recovery technique and a posteriori error estimators. Int J Numer Meth Eng 1990;30:1321–39.

[7] Mohite PM, Upadhyay CS. A simple strain recovery based a-posteriori error estimator for laminated composite plates, Technical Report no. IITK/AERO/STR/2002/01, July 2002.

[8] Pandya BN, Mallikarjuna, Kant T. Technical Report, AR&DB Board, Ministry of Defence, Government of India, 1984.

[9] Kapania RK, Raciti S. Recent advances in analysis of laminated beams and plates, Part I: shear effects and buckling. AIAA J 1989;27(7):923–34.

[10] Jones RM. Mechanics of composite materials. New Delhi: Scripta Book Company, McGraw-Hill Kogakusha, Ltd.; 1975.

[11] Herakovich CT. Mechanics of fibrous composites. New York: John Wiley & Sons Inc; 1998.

[12] Babuska I, Strouboulis T, Gangaraj SK, Upadhyay CS. Validation of recipes for the recovery of stresses and derivatives by a computer-based approach. Math Comput Model 1994;20:45–89.

[13] Zienkiewicz OC, Zhu JZ. Error estimates and adaptive refinement for plate bending problems. Int J Numer Meth Eng 1989;28:2839–53.
[14] Actis RL, Szabo BA, Schwab C. Hierarchic models for laminated plates and shells. Comput Methods Appl Mech Eng 1999;172:79–107.
[15] Oden JT, Cho JR. Adaptive hpq-finite element methods of hierarchical models for plate and shell-like structures. TICAM Report 95-16, November 16, 1995.
[16] Babuska I, Rheinboldt WC. Error estimates for adaptive finite element computations. SIAM J Numer Anal 1978;15:736–54.
[17] Babuska I, Rheinboldt WC. A-posteriori error estimates for the finite element method. Int J Numer Meth Eng 1978;12:1597–615.
[18] Bank RE, Weiser A. Some a posteriori error estimators for elliptic partial differential equations. Math Comput 1985;44:283–301.
[19] Zienkiewicz OC, Zhu JZ. A simple error estimator and the adaptive procedure for practical engineering analysis. Int J Numer Meth Eng 1987;24:337–57.
[20] Cho JR, Oden JT. A priori estimations of hp-finite element approximations for hierarchical models of plate and shell-like structures. TICAM Report 95-15, November 16, 1995.
[21] Verfurth R. A posteriori error estimators for the Stokes equation. Numer Math 1989;55:309–25.
[22] Babuska I, Plank L, Rodriguez R. Quality assessment of the a-posteriori error estimation in finite elements. Finite Elem Anal Des 1992;11:285–306.
[23] Yunus SM, Pawlak TP, Wheeler MJ. Application of the Zienkiewicz–Zhu error estimator for plate and shell analysis. Int J Numer Meth Eng 1990;29:1281–98.
[24] Pitkaranta J, Suri M. Design principles and error analysis for reduced-shear plate-bending finite elements. Numer Math 1996;75(75):223–66.
[25] Suri M, Babuska I, Schwab C. Locking effects in the finite element approximation of plate models. Math Comput 1995;64(210):461–82.
[26] Reddy YSN, Reddy JN. Linear and non-linear failure analysis of composite laminates with transverse shear. Compos Sci Technol 1992;44:227–55.